# Relaxation Time of Terahertz Magnons Excited at Ferromagnetic Surfaces

Y. Zhang (張雨),* T.-H. Chuang (莊子弘), Kh. Zakeri,† and J. Kirschner
*Max-Planck-Institut für Mikrostrukturphysik, Weinberg 2, 06120 Halle, Germany*
(Received 13 March 2012; published 24 August 2012)

The temporal and spatial properties of terahertz magnons excited at ferromagnetic fcc Co(100) and bcc Fe(110) surfaces are investigated experimentally. The magnon lifetime is found to be a few tens of femtoseconds at low wave vectors, which reduces significantly as the wave vector approaches the Brillouin zone boundary. Surprisingly, the lifetime is very similar in both systems, in spite of the fact that the excitation energy in the Co(100) film is by a factor of two larger than in the Fe(110) film. The magnon wave packets propagate only a few nanometers within their lifetime. In addition to the fact that our results describe the damping mechanism in ultrafast time scales, they may provide a way to predict the ultimate time scale of magnetic switching in nanostructures.

DOI: 10.1103/PhysRevLett.109.087203 PACS numbers: 75.30.Ds, 75.70.Ak, 75.70.Rf, 75.78.Jp

Understanding the ultrafast spin dynamics on short length and time scales is essential for increasing the density, as well as the writing or reading speed of modern magnetic storage media. Thanks to advanced experimental techniques, our knowledge has greatly improved within the last few years [1–9]. It has been known for many years that the switching of a submicron magnet typically takes place within a range of few picoseconds up to some nanoseconds, depending on the applied external magnetic field [1]. The breakthrough of the ultimate time scale of magnetic switching (up to subpicoseconds) was reported when the ultrafast optical spectroscopy was developed such that it could allow the excitation and probing of the magnetic objects [2]. Later on it was demonstrated that femtosecond laser pulses can be applied to switch the magnetization [4–7]. This new time scale seems to be the ultimate time scale of magnetic switching up to now. Interestingly, recent experimental results of spin-polarized scanning tunneling microscopy revealed that the spin relaxation time of a single magnetic atom on an insulating substrate is in the order of a few hundreds of nanoseconds [9]. A connection between the ultrafast optical spectroscopy and the results of tunneling spectroscopy is still missing. The fact is that all the techniques mentioned above allow only the investigation of the magnetic excitations in real time or space. Moreover, it is not possible to select a particular excitation with a certain wave vector and eigenfrequency and follow its dynamics. Hence a wave vector selective excitation would provide a deeper knowledge on the processes involved in the magnetic switching on ultrafast time scales.

In this Letter, we present the experimental results on terahertz magnons probed at ferromagnetic surfaces. We compare the results of Fe(110) and Co(001) and provide a quantitative analysis of the magnon lifetime at different wave vectors. We will demonstrate how the magnons are confined in time and space. Moreover, we will provide a quantitative representation of the magnons in real space.

The results are obtained using spin-polarized electron energy loss spectroscopy (SPEELS) [10], a technique which has proven its unique capability in the study of high wave vector magnons [11–13]. The unique advantage of SPEELS is that one has a direct access to the wave vector and the energy of the excitations. In the SPEELS experiments, due to the angular momentum conservation during the scattering event, magnons can only be created by electrons of minority character. The magnon peaks thus only appear in the loss region of the $I_\downarrow$ spectrum [14] (see the typical spectra in Fig. 1). The magnon excitations can be clearly identified by comparing the $I_\uparrow$ and $I_\downarrow$ spectra. The analysis of the peak position and broadening provides us information on the magnon excitation energy and lifetime, respectively [15].

We investigated the magnons in the ultrathin films of 8 monolayer (ML) fcc Co/Cu(001) and 2 ML bcc Fe/W(110). All experiments are performed at room temperature. Typical SPEELS spectra taken on 2 ML Fe/W(110) are presented in Fig. 1. As magnons can only be created by minority electrons, a magnon excitation peak appears in the $I_\downarrow$ spectrum. The difference spectrum $(I_\downarrow - I_\uparrow)$ is shown by the green curve. We note that nonmagnetic excitations, such as phonons, usually show much lower spin asymmetry [13], and will be canceled out in the difference spectrum. As the difference spectrum offers all the necessary information, it is used for further data analysis to extract the properties of magnons. To change the in-plane wave vector transfer in the measurements, the sample is rotated about the magnetic easy axis, while the angle between the incident and outgoing beams is kept fixed at 80 degrees. The in-plane components of the magnon wave vectors can be simply expressed as $\Delta k_\parallel = k_i[\sin(\theta_f) - \sin(\theta_i)]$, where $k_i$ represents the wave vector of incident electrons. $\theta_i$ and $\theta_f$ are the incident and outgoing angles, respectively. The resolution in wave vectors depends on the angular resolution of the spectrometer, which is typically about 0.05 $\text{Å}^{-1}$.

 

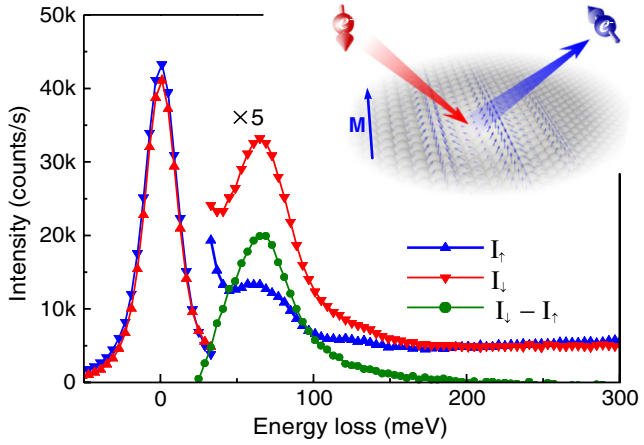


FIG. 1 (color online). Typical spectra recorded at an incident electron energy of 4 eV and a wave vector transfer of 0.6 Å$^{-1}$. The red spectrum indicates the intensity of the scattered electrons for incidence of minority electrons $I_\downarrow$, and the blue one is for the incidence of majority electrons $I_\uparrow$. The green curve is the difference between the red and blue spectra ($I_\downarrow - I_\uparrow$). The beam polarization was about 65%. The peak at about 65 meV in the red spectrum is attributed to the magnon excitations. The scattering geometry is schematically sketched in the inset.

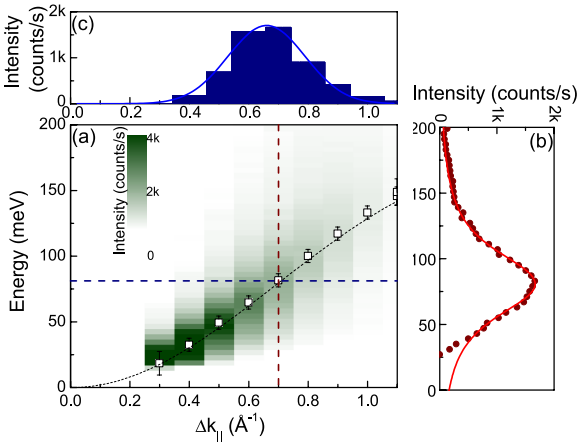


FIG. 2 (color online). (a) The difference spectra are plotted as a contour map for the wave vectors from 0 to 1 Å$^{-1}$. The section profiles for a wave vector at 0.7 Å$^{-1}$ and energy at about 82 meV are shown in (b) and (c), respectively. The magnon peak in (b) is fitted by the convolution of a Gaussian and a Lorentzian function. The intrinsic linewidth of the peak is 55 meV. The intensity profile along the horizontal line at $E = 82$ meV in (c) is fitted by a Gaussian profile shown as a solid curve.

To extract the intrinsic linewidth of the magnons, we fit the measured difference spectra by using a convolution of a Gaussian and a Lorentzian function, in which the Gaussian represents the instrumental broadening and the Lorentzian represents the intrinsic magnon signal. By fitting the experimental results, one realizes that the intrinsic linewidth of magnon excitations is typically from 20 up to a few hundreds of meV, which is usually larger than the instrumental broadening. As an example, a fit through the data shown in Fig. 1 shows that the intrinsic linewidth of the magnon is about 42 ± 7 meV, while the instrumental broadening is about 20 meV. The large broadening of the loss spectrum indicates that magnons are strongly damped in time. The magnon lifetime can be obtained from the Fourier transform of the magnon signal. The Fourier transform of the Lorentzian in energy (or frequency) domain is an exponential decay in the time domain, $\exp(-t\Gamma/2\hbar)$, where $\Gamma$ represents the intrinsic linewidth of the Lorentzian peak in energy and $\hbar$ is the reduced Planck constant. We define the lifetime of a magnon as $\tau = 2\hbar/\Gamma$, a time in which the amplitude drops to its $e^{-1}$ value. For the magnon measured on Fe(110) shown in Fig. 1, the lifetime is about 31 ± 5 femtoseconds.

The magnon intensity spectra have been measured for different wave vectors. A contour map is constructed by plotting the difference spectra versus their wave vectors for 2 ML Fe/W(110) [see Fig. 2(a)]. Figures 2(b) and 2(c) show the intensity distributions at $\Delta k_{||} = 0.7$ Å$^{-1}$ and $E = 82$ meV, respectively. If one assumes that the scattering geometry does not drastically influence the intensity in far off-specular [16], one may estimate the spatial distribution of the magnon wave packets from the intensity profile presented in Fig. 2(c). For simplicity we neglect the broadening in wave vectors due to the finite energy resolution. This is a rather good assumption, since the instrumental broadening is fairly small compared to the intrinsic linewidth. The spectral distribution as a function of the wave vector is fitted directly by a single Gaussian distribution. For example, the profile in Fig. 2(c) shows a full width at half maximum (FWHM) of about 0.32 Å$^{-1}$. After a Fourier transform, we obtained a Gaussian wave packet representing the magnon envelope function with a FWHM of about 2 nanometers.

To visualize the strong damping effects on terahertz magnons in real time and space, we compared three states of magnons for 8 ML Co/Cu(001) and 2 ML Fe/W(110). Solid symbols labeled by $S_{\mathrm{Fe}}$, $S^1_{\mathrm{Co}}$, and $S^2_{\mathrm{Co}}$ mark the centers of these states in Fig. 3(a). State $S_{\mathrm{Fe}}$ represents the magnon packet in the Fe(110) film, and states $S^1_{\mathrm{Co}}$ and $S^2_{\mathrm{Co}}$ are states in the Co(100) film. $S_{\mathrm{Fe}}$ and $S^1_{\mathrm{Co}}$ possess the same wave vector ($\Delta k_{||} = 0.8$ Å$^{-1}$), while $S_{\mathrm{Fe}}$ and $S^2_{\mathrm{Co}}$ have the same energy ($E = 100$ meV), as indicated by the dashed lines. Figure 3(b) represents the evolution of the magnon wave packets for the states $S_{\mathrm{Fe}}$, $S^1_{\mathrm{Co}}$, and $S^2_{\mathrm{Co}}$ indicated above. Each wave packet in Fig. 3(b) is the product of three components: A moving Gaussian, $\exp[-(x - vt)^2/2\sigma^2]$, representing the motion of wave packet (the envelop function), an exponential decay factor $\exp(-t/\tau)$ for the evolution of the amplitude in time, and finally a wave form, $\cos(\Delta k_{||}x - \omega t)$, representing its wavy nature ($\omega = E/\hbar$ is the angular frequency of the wave). The velocity of the envelope function, $v$, is the group velocity of the wave packet, which is obtained

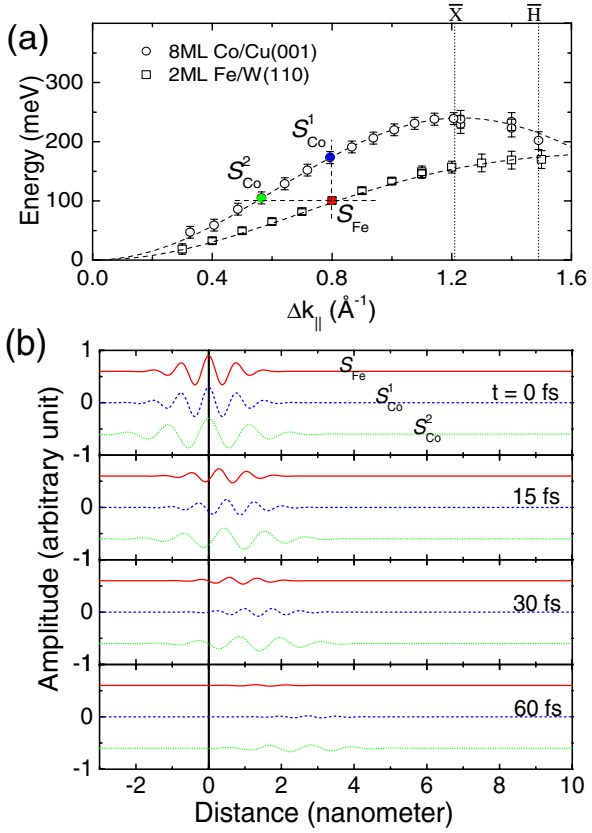


FIG. 3 (color online). (a) Magnon dispersion relation in 8 ML Co/Cu(001) (open circles) and 2 ML Fe/W(110) (open squares). Solid symbols mark the center of three states for Fe and Co surfaces, which are named as $S_{\mathrm{Fe}}$, $S^1_{\mathrm{Co}}$, and $S^2_{\mathrm{Co}}$ respectively. $S_{\mathrm{Fe}}$ and $S^1_{\mathrm{Co}}$ are at nearly the same wave vectors 0.8 Å$^{-1}$, $S_{\mathrm{Fe}}$, and $S^2_{\mathrm{Co}}$ are at almost the same energy 100 meV. The dotted lines at about 1.21 and 1.49 mark the surface Brillouin zone boundaries of Co(001) and Fe(110) surfaces. (b) The plot of the evolution of wave packets for the states $S_{\mathrm{Fe}}$ (0.80 Å$^{-1}$, 95 meV) at Fe surface, $S^1_{\mathrm{Co}}$ (0.81 Å$^{-1}$, 174 meV) and $S^2_{\mathrm{Co}}$ (0.55 Å$^{-1}$, 101 meV) at Co surface. The amplitude may be regarded as the transverse component of a precessing spin projected to the wave propagation directions or the modulus of the magnon wave function.

from the slope of the dispersion curves, $v = \partial\omega/\partial\Delta k_{\|}$. They are about 26, 46, and 41 km/s for the $S_{\mathrm{Fe}}$, $S^1_{\mathrm{Co}}$, and $S^2_{\mathrm{Co}}$ states, respectively. $\sigma$ and $\tau$ are the natural broadening of the wave packet in space and lifetime, respectively, which are obtained from the Fourier transform of the intensity spectra in Fig. 2.

In a classic picture the wave forms in Fig. 3(b) can be regarded as the amplitude of the transverse component of spins projected along a certain direction on the surface e.g., the propagation direction of the wave. It may be also regarded as the modulus of the magnon wave function. Figure 3(b) demonstrates that magnons are strongly damped within a few tens of femtoseconds and confined in a few nanometers for both Fe and Co for high wave vectors. The wave packets only moved ahead by about 2–3 nm during their lifetime (much shorter than the spin diffusion length in the 3$d$ ferromagnets). For the states from the same system i.e., $S^1_{\mathrm{Co}}$ and $S^2_{\mathrm{Co}}$, the state at a higher wave vector ($S^1_{\mathrm{Co}}$) has a shorter lifetime than the one at a lower wave vector ($S^2_{\mathrm{Co}}$). The wave packet of $S^1_{\mathrm{Co}}$ propagates a bit shorter than $S^2_{\mathrm{Co}}$. Our results demonstrate that the decay of a magnon does strongly depend on its wave vector. Interestingly, for the states on different surfaces but with similar wave vectors, i.e., $S_{\mathrm{Fe}}$ and $S^1_{\mathrm{Co}}$, it is noticed that although the $S_{\mathrm{Fe}}$ has a much lower energy, it possesses a similar lifetime and broadening of the wave packet as $S^1_{\mathrm{Co}}$. $S_{\mathrm{Fe}}$ and $S^2_{\mathrm{Co}}$ have the same energy. The state at a higher wave vector ($S_{\mathrm{Fe}}$) clearly shows a shorter lifetime as compared to the low wave vector one ($S^2_{\mathrm{Co}}$). Regarding the propagation speed, both wave packets in the Co(100) film are much faster than the ones in the Fe(110) film [see Fig. 3(b)].

The intrinsic linewidth and the corresponding lifetime of magnons versus wave vector are shown in Fig. 4 for 8 ML Co/Cu(001) and 2 ML Fe/W(110). The intrinsic linewidth of the magnon signal shows a clear dependence on the wave vector. As a result, the lifetime of magnons at the surface of 2 ML Fe/W(110) ranges from tens to hundreds of femtoseconds. Comparing to the spin relaxation of a single atom on the insulating substrate, whose relaxation time is about $10^{-7}$ s [9], the lifetime of magnons at a metal surface is almost $10^7$ times shorter. Such a short lifetime of terahertz magnons is attributed to the strong damping due to the presence of the conduction electrons in the metal film and the substrate [17–19]. Since the terahertz magnons are a coherent superposition of the correlated electron hole pairs across the Fermi level, their damping may be regarded as the result of the strong decay of these collective magnons into the available Stoner states near the Fermi level. It has been shown that the Stoner excitations in the surface states play an important role in the decay effect

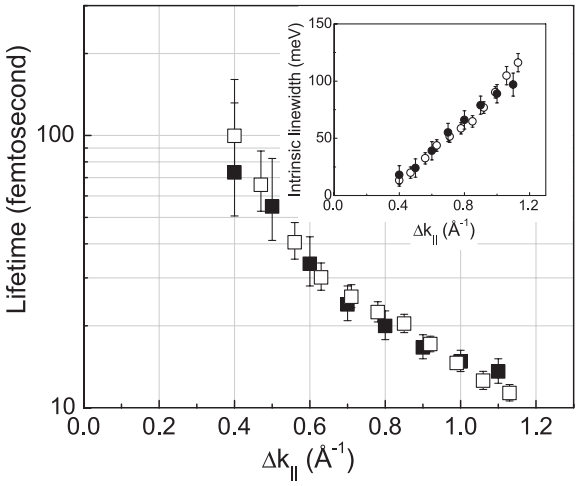


FIG. 4. The magnon lifetime as a function of the in-plane wave vector measured for 2 ML Fe/W(110) (solid symbols) and 8 ML Co/Cu(001) (open symbols). Inset shows the intrinsic linewidth of the magnon peaks.

[19–21]. If the ferromagnetic film is grown on a metallic substrate, due to the strong hybridization of the bands, there are lots of Stoner states available near the Fermi level, which can contribute to the damping mechanism. In other words, the strong decay effect may be imagined as the pumping of the spins of the magnetic film into the nonmagnetic conductive substrate [18]. It is worth pointing out that the lifetimes of both systems are very similar at the same wave vectors in spite of the fact that the magnon energy in the Co(100) film is almost twice of that in the Fe(110) film. Besides the intrinsic damping effects due to the Stoner excitations, it has been proposed that the thermal effects may also play a role in the broadening of magnon peaks [22]. However, experiments performed on a 2 ML Fe film at different temperatures revealed that the temperature dependence of the intrinsic linewidth is negligible.

The strong damping observed in our experiments is governed by the decay of collective type of magnons, to the single particle Stoner excitations (usually referred to as Landau damping [19]). It strongly depends on the available Stoner states near the Fermi level; hence, the hybridization of the electronic bands of the ferromagnetic film with the ones of the substrate plays an important role [19]. As the total magnetization of the sample is unchanged after creation and damping of a magnon, one cannot directly connect the magnon lifetime to the ultimate time scale of magnetization switching. However, this relaxation time can be directly compared to the time interval provided in the excitation scheme. For instance, if the aim is to switch the magnetization of a nanoisland using a spin-polarized current within a few femtoseconds, the terahertz magnons are governing this process. Hence, the time interval between two electrons has to be shorter than the lifetime of the magnons involved. Otherwise, the magnons do not contribute to this switching process and die out. The same analogy applies to the other methods used to switch the magnetization. If terahertz magnons are generated within the process, one would expect the response of the system in such timescales. Since the timescale in optical experiments is similar to what we predict as the typical lifetime of the terahertz magnons, we think that the terahertz magnons are also important in the laser induced demagnetization processes.

The strong spin dependence of the decay rate of the image potential state observed in photoemission experiments is attributed to the magnon generation and relaxation within a few tens of femtoseconds [23]. Our results are the direct experimental proof of this hypothesis.

In summary, the magnon lifetime and spatial distribution in 8 ML fcc Co(001) and 2 ML bcc Fe(110) are studied. The magnons on both surfaces possess lifetimes ranging from tens to hundreds of femtoseconds depending on the wave vector. Our analysis reveals that the magnons at the Fe(110) and Co(100) surfaces are strongly confined in time and space due to the damping effects. Interestingly, the lifetime of both systems are very close at a given wave vector in spite of the fact that the excitation energy in the Co(100) film is almost twice of that in the Fe(110) film. Terahertz magnons propagate only a few nanometers within their lifetime. Our results shall have a significant contribution to the understanding of the magnetic damping mechanism of terahertz magnons at surfaces and a possible tuning of the magnetic relaxation in nanoscale ferromagnets. They may also offer a way of estimating the ultimate time scale of magnetic switching in nanostructures.

We acknowledge the fruitful discussions with P. Buczek and L. M. Sandraskii. We thank W.-X. Tang, J. Prokop and M. Etzkorn for their contribution to some experiments.

*zhangyu@mpi-halle.de
†zakeri@mpi-halle.de

[1] *Spin Dynamics in Confined Magnetic Structures II*, edited by B. Hillebrands and K. Ounadjela (Springer, Heidelberg, 2003).
[2] E. Beaurepaire, J.-C. Merle, A. Daunois, and J.-Y. Bigot, Phys. Rev. Lett. **76**, 4250 (1996).
[3] I. Tudosa, C. Stamm, A. B. Kashuba, F. King, H. C. Siegmann, J. Stöhr, G. Ju, B. Lu, and D. Weller, Nature (London) **428**, 831 (2004).
[4] C. D. Stanciu, F. Hansteen, A. V. Kimel, A. Kirilyuk, A. Tsukamoto, A. Itoh, and Th. Rasing, Phys. Rev. Lett. **99**, 047601 (2007).
[5] U. Bovensiepen, J. Phys. Condens. Matter **19**, 083201 (2007).
[6] B. Koopmans, G. Malinowski, F. Dallla Longa, D. Steiauf, M. Fähnle, T. Roth, M. Cinchetti, and M. Aeschlimann, Nature Mater. **9**, 259 (2010).
[7] A. Kirilyuk, A. V. Kimel, and T. Rasing, Rev. Mod. Phys. **82**, 2731 (2010).
[8] M. Fähnle and C. Illg, J. Phys. Condens. Matter **23**, 493201 (2011).
[9] S. Loth, M. Etzkorn, C. P. Lutz, D. M. Eigler, and A. J. Heinrich, Science **329**, 1628 (2010).
[10] H. Ibach, D. Bruchmann, R. Vollmer, M. Etzkorn, P. S. Anil Kumar, and J. Kirschner, Rev. Sci. Instrum. **74**, 4089 (2003).
[11] R. Vollmer, M. Etzkorn, P. S. Anil Kumar, H. Ibach, and J. Kirschner, Phys. Rev. Lett. **91**, 147201 (2003).
[12] W. X. Tang, Y. Zhang, I. Tudosa, J. Prokop, M. Etzkorn, and J. Kirschner, Phys. Rev. Lett. **99**, 087202 (2007).
[13] Y. Zhang, P. A. Ignatiev, J. Prokop, I. Tudosa, T. R. F. Peixoto, W. X. Tang, Kh. Zakeri, V. S. Stepanyuk, and J. Kirschner, Phys. Rev. Lett. **106**, 127201 (2011).
[14] M. Plihal, D. L. Mills, and J. Kirschner, Phys. Rev. Lett. **82**, 2579 (1999).
[15] M. Etzkorn, P. S. Anil Kumar, and J. Kirschner, *Handbook of Magnetism and Advanced Magnetic Materials* (John Wiley & Sons, New York, 2007) Vol. 3, p. 1658.
[16] H. Ibach and D. L. Mills, *Electron Energy Loss Spectroscopy and Surface Vibrations* (Academic Press, New York, 1982).

[17] A. T. Costa, R. B. Muniz, and D. L. Mills, Phys. Rev. B **68**, 224435 (2003).
[18] A. T. Costa, R. B. Muniz, and D. L. Mills, Phys. Rev. B **74**, 214403 (2006).
[19] P. Buczek, A. Ernst, and L. M. Sandratskii, Phys. Rev. Lett. **106**, 157204 (2011).
[20] T. Balashov, T. Schuh, A. F. Takács, A. Ernst, S. Ostanin, J. Henk, I. Mertig, P. Bruno, T. Miyamachi, S. Suga, and W. Wulfhekel, Phys. Rev. Lett. **102**, 257203 (2009).
[21] A. A. Khajetoorians, S. Lounis, B. Chilian, A. T. Costa, L. Zhou, D. L. Mills, J. Wiebe, and R. Wiesendanger, Phys. Rev. Lett. **106**, 037205 (2011).
[22] A. Taroni, A. Bergman, L. Bergqvist, J. Hellsvik, and O. Eriksson, Phys. Rev. Lett. **107**, 037202 (2011).
[23] A. B. Schmidt, M. Pickel, M. Donath, P. Buczek, A. Ernst, V. P. Zhukov, P. M. Echenique, L. M. Sandratskii, E. V. Chulkov, and M. Weinelt, Phys. Rev. Lett. **105**, 197401 (2010).